modelling

MDPI

Article

Development of a Methodology for Obtaining Solid Models of Products That Are Objects of Reverse Engineering Using the Example of the Capstone Micro-GTU C 65

Sergey Osipov, Ivan Komarov, Olga Zlyvko, Andrey Vegera and George Gertsovsky *

Department of Innovative Technologies of High-Tech Industries, Institute of Energy Efficiency and Hydrogen Technologies, National Research University "Moscow Power Engineering Institute", 111250 Moscow, Russia; osipovsk@mail.ru (S.O.); komarovii@mpei.ru (I.K.); zlyvkoov@mpei.ru (O.Z.); vegeraan@mpei.ru (A.V.)
* Correspondence: gertsovskyga@mpei.ru

Abstract: Currently, about a thousand micro gas turbine units of small and medium capacity are in operation in the Russian Federation, which are used as an autonomous power source at critical infrastructure facilities. During long-term operation, the component parts of the micro GTU may fail and require replacement or repair. The lack of spare parts and design documentation for their production makes it impossible to operate. As a way to solve the problem, the reverse engineering process can be used to produce components. One of the stages of reverse engineering is to determine the geometric parameters of the object. The fastest and most accurate way to obtain geometric characteristics in the reverse engineering process is 3D scanning. Three-dimensional scanning technology is used to obtain a solid 3D model of the prototype surface, based on which design documentation is subsequently developed. This article presents the results of a study of the influence of the parameters of the distance between polygonal grid points and the scanner exposure on the detailing of the outer surface and the geometric parameters of the resulting polygonal model. As a result of this study, the dependence of the final file size and the time spent on scanning and processing on the distance between the points of the polygonal grid and the model was established. Based on the dependence of the parameters, recommendations were obtained for choosing the distance between the points of the polygonal grid of laser 3D scanning. Also, after performing the stages of reverse engineering, the methodology for creating solid models and design documentation of parts of power equipment units using 3D scanning technology was improved.

Keywords: 3D modeling; 3D scanning; combustion chamber; reverse engineering; point cloud; polygonal modeling

Citation: Osipov, S.; Komarov, I.; Zlyvko, O.; Vegera, A.; Gertsovsky, G. Development of a Methodology for Obtaining Solid Models of Products That Are Objects of Reverse Engineering Using the Example of the Capstone Micro-GTU C 65. *Modelling* **2024**, *5*, 1980–2000. https://doi.org/10.3390/modelling5040103

Academic Editor: Josef Kiendl

Received: 24 September 2024
Revised: 7 November 2024
Accepted: 26 November 2024
Published: 6 December 2024

1. Introduction

Gas turbine units are used in various industrial fields to provide electricity and heat. Micro gas turbine units of small and medium power are used as an autonomous power source and infrastructure facilities [1]. Units from the American company Capstone make up about 70% of the total number of imported micro gas turbine units used in the Russian Federation [2].

Due to the lack of official representation of foreign manufacturing companies, the supply of components for micro-GTUs requires more time. The problem of replacing components for equipment in a short time can be solved using reverse engineering methods. One of the main tasks in the reverse engineering process is to obtain geometric parameters that are used to develop a solid 3D model of the product. Obtaining geometric parameters is possible using contactless and contact methods of interaction with the prototype of the part. Contact methods are usually used for simple-shaped parts, which use measuring instruments. For complex-shaped parts, contactless 3D scanning methods are used to obtain their surface in the form of a point cloud.

Three-dimensional scanning is a method of obtaining data on the shape and dimensions of an object in spatial representation by recording the x, y, and z coordinates of points on the surface of the object and converting the set of points into an electronic geometric model using specialized software [3].

There are various types of 3D scanning, which are classified into contact and non-contact. When using contact methods, it is necessary to interact directly with the surface of the product to obtain its geometric characteristics. The contact method of 3D scanning includes the device of a coordinate measuring machine (CMM), which is widely used in production. The disadvantage of this type of scanning is that it requires physical contact with the object, which is impossible for valuable or fragile items. Application of the CMM method requires more time than other methods, due to the slow movement of the prob and that is how the scanned surface is obtained [4].

Among the contactless methods of 3D scanning in industry, laser and light scanners are widely used, which use installed sensors and cameras during scanning due to which an image of the scanned object is obtained. Then, the obtained images are analyzed using the built-in scanner software, which calculates the coordinates of points on the surface of the product and creates a point cloud in the form of the scanned surface [5,6]. For laser scanners, unlike light scanners during 3D scanning, reflective marks must be applied to the surface of the scanned prototype to orient the point cloud relative to the coordinates of the scanner processing program (xyz) [7].

Also, improved methods of processing the obtained data using machine learning are currently being used to improve the results of the 3D scanning process of various objects.

Thus, in the work [8], a method is proposed that allows taking into account the problems associated with light reflection in the forecasting process. In addition, studies related to the prediction of deviations during scanning were carried out to reduce surface deviations [9].

These methods use built-in functions to predict and analyze the data obtained. It is noted that one of the methods for forecasting that has proven itself and shown high efficiency is the Kolmogorov–Arnold Network (KAN) method [10], which provides exceptional accuracy and predictability, making it a promising alternative to predictive modeling in various fields.

The main stages of 3D scanning include analysis and preparation of the product surface scanning, editing and post-processing of the resulting point cloud, creation of a polygonal model, and development of a solid model based on a polygon mesh [11,12].

In the studies [13,14], reverse engineering methods were used to create solid models of the Francis hydraulic turbine. The resulting solid models of equipment parts were then used to simulate and study the flow guide using computational fluid dynamics (CFD) tools.

In [15], the possibility of reconstructing the geometric parameters of steam turbine blades using 3D scanning was investigated. An important requirement was to preserve the specified strength and geometric characteristics. Since the selected blade samples had external surface defects, the nominal dimensions were obtained from the average values of several scanned models.

In the study [16], 3D structural light scanning technology was used to obtain the geometry of the steam turbine rotor stage blades. The obtained blade profile geometry was used to create solid models of the steam turbine disks. The resulting solid model was then used to simulate the dynamic analysis of the steam turbine rotor.

In the work [17], the possibility of increasing the efficiency of a micro gas turbine unit that is used to generate electricity using a solar thermal power plant was investigated. To obtain a solid model of the micro gas turbine compressor part, due to its complex external profile, the technology of structural-light 3D scanning was used. Subsequently, the obtained solid model of the compressor created on the basis of a polygonal mesh was used for modification. The modification was made on the basis of the obtained solid model by changing the geometry of the external profile. Also, the basic and modified solid models were used for CFD modeling.

Based on the results of the review, it was determined that there are currently no detailed methodological recommendations for 3D scanning of power equipment parts, and the influence of 3D scanning parameters on the detailing and geometric characteristics of power equipment units of small and medium-capacity gas turbine units has not been established.

In this paper, the influence of various parameters of the 3D scanning process on the geometric characteristics of the scanned surface of the product was investigated, and a method for obtaining solid 3D models of parts that are objects of reverse engineering was developed.

2. Materials and Methods

2.1. Object of Study

The Capstone micro gas turbine unit was chosen as the object of study: C 65, 65 kW electric power. The main characteristics of the Capstone micro-GTU C 65 are presented in Table 1 [18].

Table 1. Main technical characteristics of the Capstone micro-GTU C 65 [18].

Parameter	Value
Nominal electric power, kW	65
Efficiency by electricity, %	28
Overall efficiency of power plant (with heat recovery), %	up to 90
Length × width × height, mm	1516 × 762 × 1943
View fuel	gas, kerosene, diesel

The Capstone Micro-GTU combustion chamber housing the C 65 consists of several parts, as shown in Figure 1. On the shell (housing) (1) of the combustion chamber, there are 6 holes for feeding fuel into the mixing zone. At the same time, special adapter plates (3) are made for four holes inside. The fixing outer flange (2) is to ensure thermal expansion of the combustion chamber, which occurs due to the temperature difference. Two holes for injectors without adapter plates are located symmetrically because the combustion chamber body is fixed inside the micro-GTU unit.

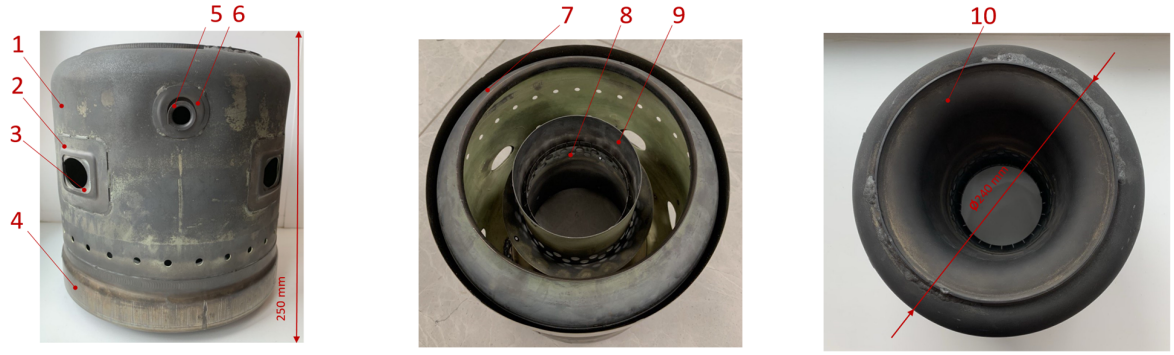

(**a**) (**b**) (**c**)

Figure 1. Components of the combustion chamber housing of the Capstone micro-GTU C 65: (**a**) main view, (**b**) view of the combustion chamber body from below, (**c**) view of the combustion chamber body from below. 1—shell (body), 2—outer flange, 3—adapter plate, 4—shell lower, 5—adapter plate, 6—external flange, 7—bottom, 8—lower funnel, 9—lower branch pipe, 10—funnel.

At the bottom of the combustion chamber, there is a lower shell part (4). At the level of the holes for the injector without external flanges, there is a hole for the spark plug. To install the spark plug, the design provides parts of the adapter plate (5) and the fixing external flange (6).

On the combustion chamber body part, there is a row of holes through which the air mixture is supplied. On the lower side of the body, there are parts of the bottom (7), the lower funnel (8) with two rows of mixing holes, and the lower branch pipe (9). Inside the body, there is a funnel part (10).

On the combustion chamber of the Capstone micro-GTU C 65, we found surface defects that arose during operation for 25,000–35,000 h. The most noticeable deformations were found on the body part (1), as shown in Figure 2. The deformations of the parts were taken into account in the process of obtaining the polygonal model and when creating a solid 3D model.

Figure 2. Deformations of combustion chamber parts of the Capstone micro-GTU C 65 of the housing part near the injector holes.

2.2. Research Methodology

The methodology for creating a solid 3D model and sketch design documentation for the combustion chamber housing of the Capstone C 65 micro turbine was based on previous studies presented in [19]. This methodology was enhanced by adding additional interaction blocks. Unlike the initial scheme, a stage was added to determine the optimal brightness parameters when scanning markers for positioning. Additionally, a block for setting the distance parameter between points of the polygonal mesh was added to achieve a more detailed scanned surface.

The flowchart of the methodology was divided into two main stages: (1) obtaining a polygonal model based on data acquired during 3D scanning, and (2) processing polygonal and solid models obtained in the reverse engineering process, as shown in Figures 3 and 4 («+» Condition block satisfied, «—» Condition block not satisfied).

Initially, an analysis and preparation of the camera housing were conducted, during which the component parts of the housing, surface defects, and potential hard-to-scan areas were identified. At this stage, the sample of the combustion chamber housing was cleaned of abrasive materials and dust to apply markers used for positioning the item relative to the scanner program's base coordinates, as shown in Figure 5.

The Shining 3D FreeScan UE Pro scanner was used as equipment for the 3D scanning process and the study of the effect of the set settings on the detail of the outer surface and geometric parameters of the polygonal model of the combustion chamber housing of the Capstone C 65 micro-GTU. The characteristics of the FreeScan UE Pro handheld laser scanner are presented in Table 2 [20].

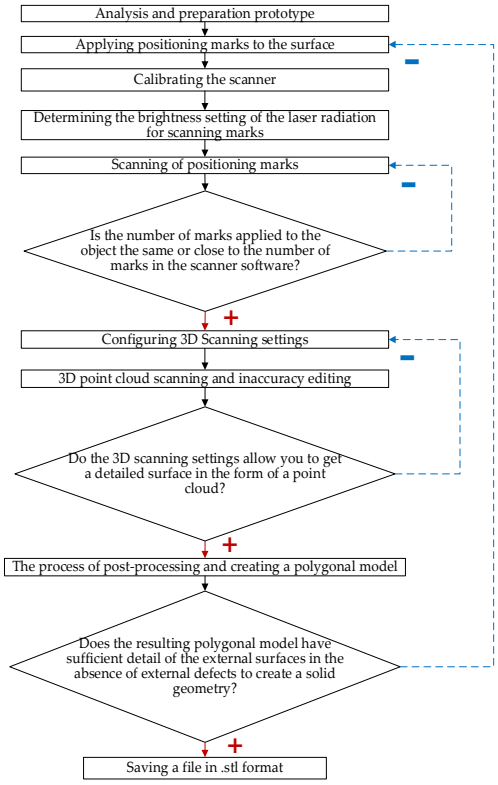

Figure 3. Flowchart of an improved methodology for creating preliminary design documentation for the Capstone C 65 gas turbine plant (stage 1—obtaining a polygonal model).

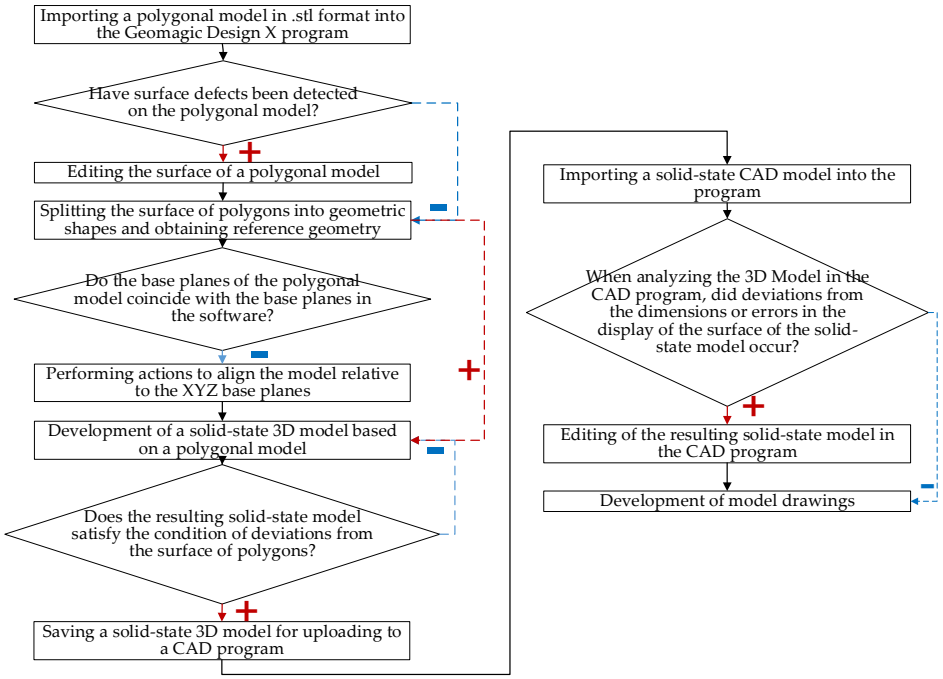

Figure 4. Flowchart of an improved methodology for creating preliminary design documentation for the Capstone C 65 gas turbine unit (stage 2—processing of the polygonal and solid-state models).

Figure 5. The combustion chamber body of the Capstone micro-GTU prepared for the 3D laser scanning process C 65 with reflective markings applied.

Table 2. Technical characteristics of the Shining 3D laser scanner FreeScan UE Pro [20].

Parameter	Value (Mode)	
Mode scanning	Mode grids, one line	7 parallel lines
Accuracy scanning, mm	>0.02	
Speed scanning, dots/s	1,850,000	
Maximum range scanning, mm	600 × 550	
Optimal distance scanning, mm	300	200

A personal computer (PC) Graviton D50A was used as equipment for processing the received data obtained during 3D scanning. The characteristics of the PC Graviton D50A are presented in Table 3.

Table 3. Characteristics of the PC Graviton D50A.

Component	Specification
Processor	AMD Ryzen 7 5700X, 8 Core
Video card	NVIDIA GeForce RTX 3060, 8 GB
RAM	32 GB
System type	Windows 10, ×64

Before the scanning of the markers, the scanner was calibrated under external light sources. It was ensured that the external lighting remained constant, as this factor could affect the detailing and accuracy of the polygonal model.

During the scanning process, a 3D laser scanner emits a pattern in the form of a grid or lines onto the surface of the product. By means of built-in cameras, the distance and position of each point on the scanned surface are determined by changing the grid when the scanner moves. This interaction occurs using the triangulation process, in which the laser source, the scanner cameras, and the product form a triangle to determine the distance to the object, as shown in Figure 6. As a result of scanning the external and internal geometry of the product, a three-dimensional digital image of the object is created in the form of a point cloud.

The advantage of using a laser scanner over others is its high accuracy (up to 20 μm) and scanning speed. Also, in most cases, laser scanning, unlike light scanning, does not require additional matting of external reflective surfaces [21].

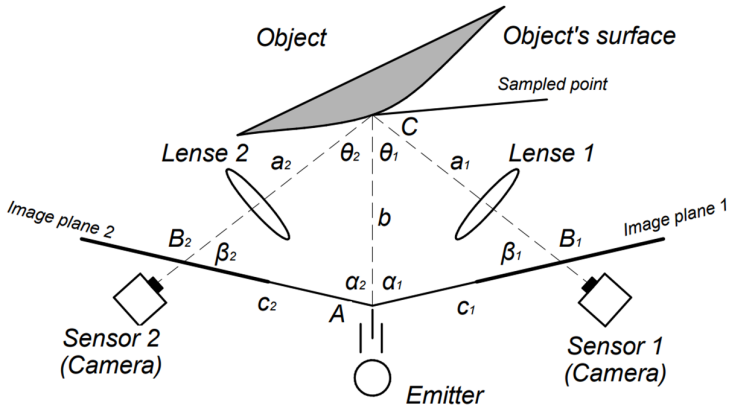

Figure 6. Operating principle of a 3D laser scanner.

As settings for laser 3D scanning, it is possible to use various modes of displaying laser radiation on the surface of an object, set the distance between points of a polygonal grid, select the type of surface being scanned, and set the exposure setting. All laser scanner settings are set using the FreeScan scanner software (V2.0.1.2).

For 3D scanning of the surface, different modes of laser beam display on the product surface were used. Three modes are available for the 3D laser scanning process: grid mode, seven parallel lines mode, and single line mode, as shown in Figure 7. The choice of laser beam display mode affects the speed and accuracy of scanning.

(**a**) (**b**) (**c**)

Figure 7. Modes for displaying the radiation source during 3D laser scanning: (**a**) light source—grid, (**b**) light source—seven parallel lines, (**c**) light source—single line.

When using the grid beam mode, most of the surface is scanned, but it is more difficult to obtain more detailed surfaces near edges or holes. In this case, the seven parallel lines or single line beam modes are used to increase the detail of certain elements.

During 3D scanning of the combustion chamber body, the following settings were used: distance between points, type of scanned surface, exposure value, and laser radiation source mode. During the study of scanning parameters for detailing the combustion chamber polygonal model, the distance and exposure values were changed. During 3D scanning, the time spent on scanning and post-processing to obtain a polygonal model, the number of frames during mesh construction, the number of points, and the final size of the STL-file were recorded for each experiment.

After laser 3D scanning of the entire surface of the product, a post-processing process was carried out, in which a polygonal model of the combustion chamber housing of the Capstone C 65 micro-GTU was obtained based on the scanned point cloud. The resulting polygonal model of the combustion chamber housing of the Capstone C 65 micro-GTU was used to create a solid 3D model in the Geomagic program Design X; then, based on the

obtained solid model of the combustion chamber body, a draft design documentation was developed.

3. Results and Discussions

3.1. Study of the Influence of 3D Scanning Parameters on the Detail and Geometric Characteristics of a Polygonal Model

Before starting the 3D laser scanning, three experimental scans of the positioning marks were performed at different brightness parameters. Marker scanning, unlike point cloud scanning, is performed by photogrammetry. Brightness parameters that are incorrectly determined when scanning markers affect the speed of the marker display process in the scanner program, as shown in Figure 8.

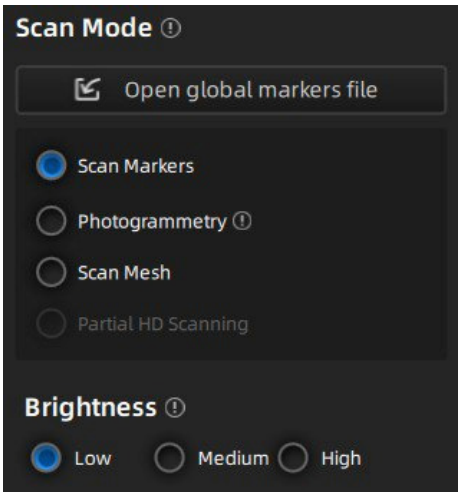

Figure 8. Selecting the brightness setting when scanning markers on the surface of the combustion chamber of the Capstone C 65 micro-GTU.

In addition, if the brightness is insufficient, not all marks on the surface can be scanned, which may affect the 3D laser scanning process. In real production conditions, the brightness parameter for scanning markers is determined depending on the reflectivity of the surface of the scanned prototype, as well as depending on the complexity of the product profile.

A total of 125 marks were applied to the entire outer surface of the Capstone micro-GTUC 65 combustion chamber housing. After scanning the labels, it was found that the best display result, in which all the labels applied to the body were displayed in the scanner program, was achieved at average brightness settings of the radiation source. Scanning of positioning marks, unlike the 3D laser scanning process itself, was performed using the built-in photogrammetry method.

To study the settings of laser 3D scanning, the settings that have the greatest impact on the scanning process were used. The exposure parameters and the specified distance between the points of the polygonal grid had the greatest impact on the scanning process. When the exposure setting is reduced, the brightness of the laser grid display decreases, due to which the scanning process may be interrupted, since the scanner does not recognize the grid on the surface of the object. Also, when the exposure is reduced, the deviation of the grid is less noticeable, which affects the detailing of the surface of the polygonal model. Setting the distance between the points of the polygonal grid affects the detailing of the scanned surface and the accuracy of the display. With a specified setting of the distance between the polygonal grid of less than 0.5 mm, the size of the polygonal model file can be significantly increased. Therefore, by reducing the distance between the points of the polygonal grid to less than 0.5 mm, the final time of the full cycle of developing a 3D model with limited computing power can increase.

To obtain the first test polygonal model, the distance between the points of the polygonal grid was set to 1 mm. The first experimental scanning was carried out to determine the settings and modes at which the time for obtaining the polygonal model would be minimal with satisfactory detailing of the scan surface. To increase the scanning speed, the distance between the points of the polygonal model was set to 1 mm. The exposure setting was set at 30% of the maximum value, since when using the automatic exposure determination function, the value is set in the range from 25 to 30%. Automatic exposure determination was not used in the study, since at the beginning of each pass, determining the exposure parameter additionally takes from 2 to 3 min. Three laser radiation display sources were used during scanning. Initially, a laser radiation source in the form of a grid was used to scan most of the case surface. Then, to smooth out transition parts and scan the surface near the holes, the laser radiation mode in the form of seven parallel lines was first used, after which a laser radiation source in the form of a single line was used for the final scanning of the darkened surface.

Scanning the outer surface of the combustion chamber of the Capstone micro-GTU C 65 was completed in five passes. One pass means the maximum possible filling of the point cloud with the given scanner parameters and the given unchangeable position of the scanned object before saving and editing it. The resulting polygonal model as a result of the first experiment was obtained in 47 min but had mediocre detailing in the presence of external surface defects in the form of overlapping surfaces of the polygonal mesh, as shown in Figure 9a.

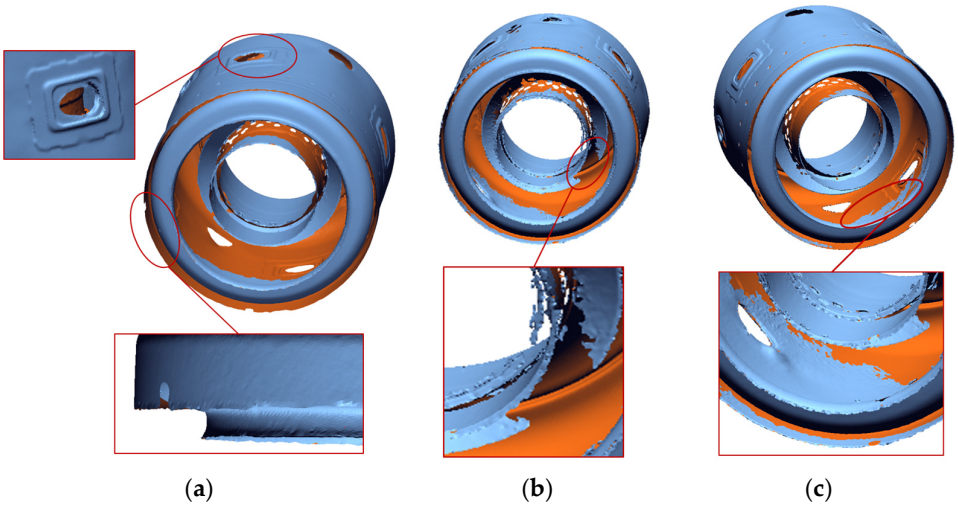

Figure 9. Surface defects of scanned polygonal models of the combustion chamber housing of the Capstone micro-GTU C 65: (**a**) surface defects of the first polygonal model; (**b**) surface defects of the second polygonal model; (**c**) surface defects of the third polygonal model.

To obtain the second polygonal model, the distance between points was set to 0.5 mm. The exposure setting was set at 25% of the maximum value. To digitize all surfaces of the combustion chamber body, seven scanner passes were performed along the surface using different laser radiation display modes, similar to the first experiment. After post-processing and obtaining a polygonal model of the combustion chamber body of the Capstone micro-GTU C 65, defects in the form of small unfilled areas were noticeable, as shown in Figure 9b. Based on the results of the second experiment, it was suggested that in order to increase the detail of the outer surface, it is necessary to further reduce the distance between the points of the polygonal mesh.

The third experimental scan took into account the defects in the form of an unfilled mesh surface resulting from obtaining the second polygonal model. The distance between points was reduced to 0.3 mm, and the exposure settings were set at 25% of the maximum value. The scan was performed in seven passes using different laser radiation display sources, similar to the first experiment. After editing the point cloud and post-processing, a

surface defect in the form of a double overlap of the polygonal mesh of the outer and inner parts of the body was formed on the surface of the obtained polygonal model, as shown in Figure 9c.

In the fourth experimental scan, it was decided to change the distance between points to 0.2 mm to improve the quality of the surface scan and eliminate surface defects of the polygonal model. The exposure setting was set at 30% of the maximum value, since it was noted that the brightness of the laser source was insufficient for 3D scanning of darkened internal surfaces. Scanning the entire surface of the combustion chamber housing of the Capstone micro-GTU C 65 was performed in seven passes, with different laser sources. This scanning allowed us to obtain a more complete view of the surface without obvious defects and overlaps. The obtained results of the study of the influence of scanning parameters on the time spent and the characteristics of the polygonal model are shown in Table 4.

Table 4. Results of the study of the influence of laser 3D scanning settings of the combustion chamber housing of the Capstone micro-GTU C 65.

No.	Setting Parameter Exposures, %	Distance Between Dots, mm	Scanning and Processing Time, min.	Number of Frames to Build	Quantity Dots	Size STL-File, Kb
1	30	1.0	47	45,123	566,363	28,867
2	25	0.5	95	73,406	5,873,551	256,925
3	25	0.3	87	75,409	6,082,865	399,400
4	30	0.2	58	74,999	7,939,372	922,431

In the process of 3D scanning, at a given distance between points of less than 0.2 mm, the filling limit for points on the surface was determined to be 10,800,000 points. Due to the specified software limitations, it is not possible to obtain a more detailed surface when using this equipment. When an additional scan of the outer surface is attempted, when the limit is reached, the surface is filled only at the point of contact of the grid, and in other places, the surface detail decreases. This information should be taken into account when scanning larger parts.

Based on the conducted research, the best result was obtained with the fourth experimental scanning with an exposure setting of 30% of the maximum and a specified distance between points of 0.2 mm. As a result, after a complete scan of the Capstone C 65 micro-GTU housing, the polygonal model had sufficient detailing of the outer surface near the holes and edges, as shown in Figure 10. It was also possible to increase the speed and reduce the scanning time by 30–37 min compared to the second and third experiments.

Based on the research data, dependencies were obtained between the distance between the points of the polygonal grid on the final file size and on the time required for scanning and processing, as shown in Figure 11. Analysis of the obtained dependence shows that when the distance between points decreased from 1 to 0.4 mm, the file size of the polygonal model increased linearly (a decrease of every 0.1 mm in the distance between points led to an increase in the file size by 1.3 times and the time for scanning and processing by 1.2 times).

When the distance decreased to less than 0.35 mm, the file size grew exponentially. Thus, when the distance decreased from 0.3 to 0.2 mm, the file size increased by 2.3 times.

When analyzing the dependence of the selected distance between the points of the polygonal grid on the final time required for scanning and processing, it was noted that with a selected distance between the points from 1 to 0.4 mm, the time spent increased by 1.3 times with a decrease in distance by every 0.1 mm. With a given distance of less than 0.35 mm to 0.2 mm, the time spent decreased by 1.5 times.

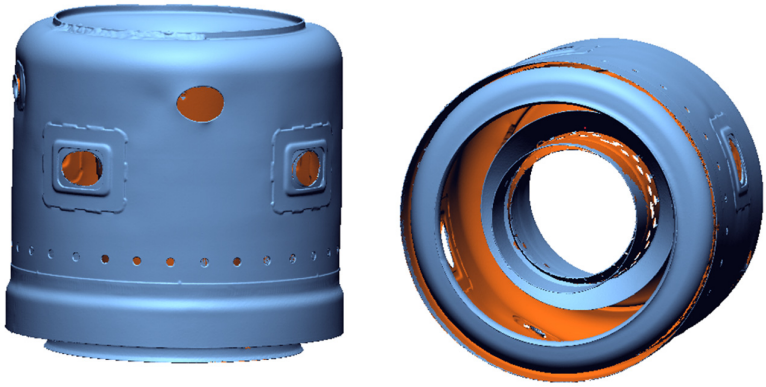

Figure 10. The resulting polygonal model of the combustion chamber housing of the Capstone micro-GTU 65 after the fourth scan.

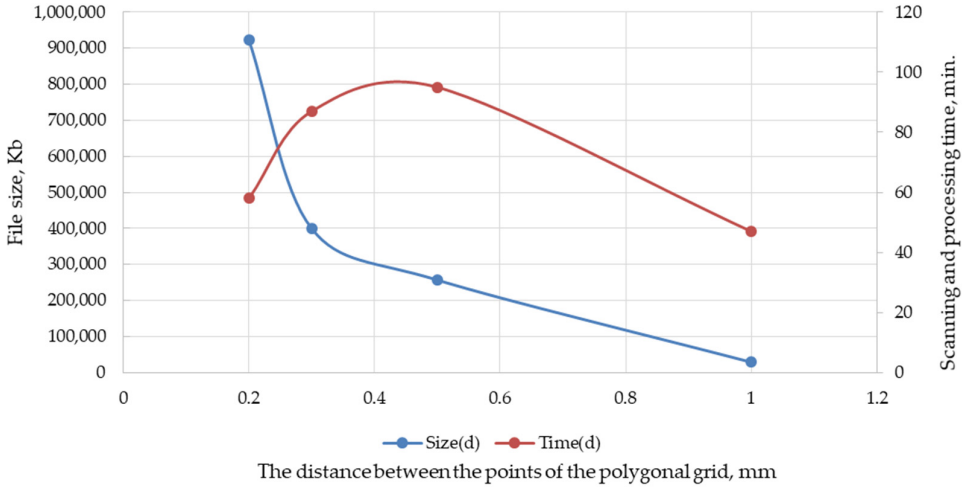

Figure 11. Dependence of the distance between points of the polygonal mesh on the final size of the polygonal model file and the total time spent on scanning and processing the polygonal model.

3.2. Development of a Solid Model of the Combustion Chamber

Geomagic software Ver 2022.0.0 was used to obtain a solid model of the combustion chamber based on its polygonal model, Design X. When creating the solid geometry, the polygonal model of the combustion chamber body of the fourth experimental scan obtained at the previous stage of the study was used.

To obtain a solid 3D model of the combustion chamber of the Capstone C 65 micro-GTU, the surface of the polygonal model was divided in accordance with the product details described earlier.

Initially, when creating solid geometry, it was necessary to select a base part relative to which the dimensionality of all solid bodies would be built, since when aligning a polygonal model relative to the base coordinates of the Geomagic program Design X by (XYZ) dimensions, deviations may occur due to external defects in the surface of the scanned product or the scanned polygonal mesh.

To create sketches when setting the dimensions of Capstone C 65 micro-GTI solid parts, the mesh sketch function of the Geomagic Design X program was used, with which one can create a sketch contour using the surface of a polygonal model. The contour of the scanned polygon surface, which was used to create the sketch, is highlighted in purple, as shown in Figure 12.

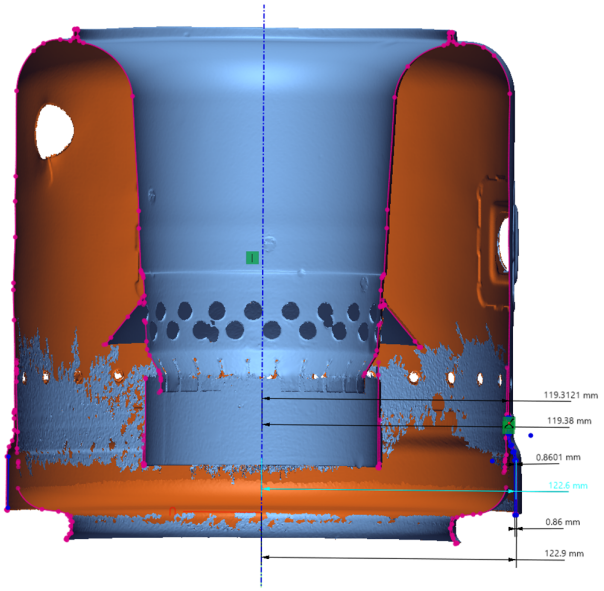

Figure 12. Creating a sketch to obtain a solid-state model of the lower shell using the built-in mesh sketch function.

Before the start of development, the thickness of each part was determined using the measuring tools of a caliper and a micrometer. It was found that all parts had the same thickness of 21 Gauge (0.874 mm), in accordance with the US standard gauge for rolled steel [22]. This thickness size was set during construction for each part of the combustion chamber.

The bottom shell part was chosen as the base part, since it had the smallest deformations and surface deviations caused by thermal deformations. After applying the main dimensions to the sketch, a solid geometry of the bottom shell was created. To analyze the dimensional deviations from the polygon surface, each solid part was checked using the built-in Geomagic function Design X "Body Deviation". If the part had deviations greater than 1 mm (0.0393 in), the sketch dimensions were changed to obtain the smallest deviation, as shown in Figure 13.

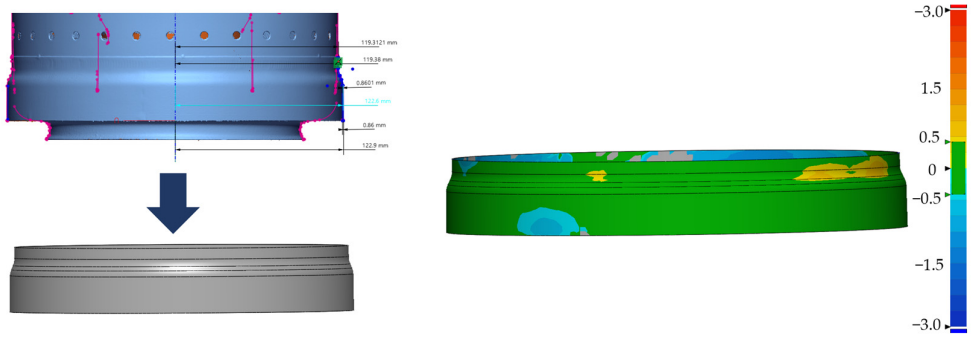

(**a**) (**b**)

Figure 13. Receipt and inspection of solid parts of the combustion chamber housing of the Capstone micro-GTU C 65 in the Geomagic program Design X: (**a**) creating solid geometry from a polygonal mesh; (**b**) checking deviations of the solid part from the polygonal model using the Body Deviation function.

Initially, the solid-state geometry of the combustion chamber part was created relative to the base planes of the Geomagic Design X program during development. The base planes were determined as a result of the alignment of the polygonal model relative to the base coordinates. Due to the use of base planes, the deviations of the solid-state housing

model turned out to be too large in the range from −3.92 mm to 3.147 mm, as shown in Figure 14.

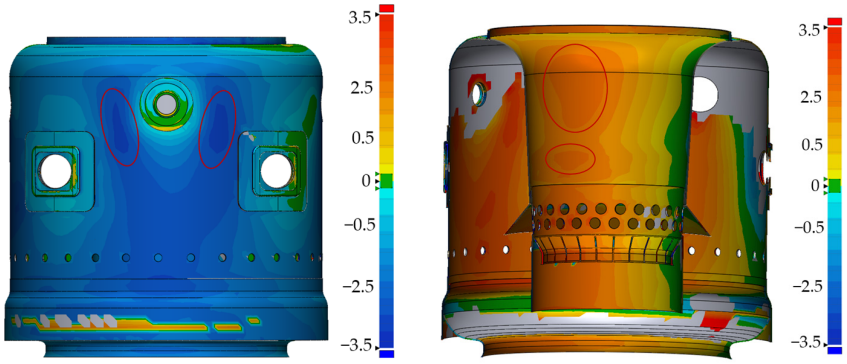

(**a**) (**b**)

Figure 14. The deviations obtained during the development of the initial solid-state model of the combustion chamber housing micro-GTU Capstone C 65 (Areas of greatest deviations highlighted in red): (**a**) the value of the smallest deviation on the body part; (**b**) the value of the largest deviations on the funnel part.

During the re-development of the 3D model, each part of the combustion chamber was created relative to the body part, which reduced deviations from the polygon surface from −0.5 to 0.5 mm for the parts.

Next, all the components of the combustion chamber body of the Capstone C 65 micro-GTU were obtained in the form of solid 3D models. For each body part, the deviations of the sizes from the surface of the polygonal mesh were analyzed, by analogy with the lower shell part. The dimensional deviations of the solid 3D models of the combustion chamber body parts of the Capstone C 65 micro-GTU from the surface of the polygonal mesh are shown in Table 5.

Table 5. Deviation of the dimensions of solid 3D models of the combustion chamber body parts of the Capstone micro-GTU C 65 from the surface of the polygonal mesh.

Name Details	Contours Deviations	Deviations from the Surface of the Polygonal Mesh, mm
Shell lower	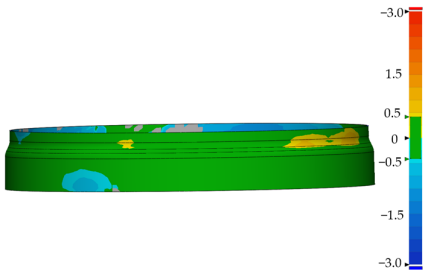	from −0.688 to 0.62
Funnel	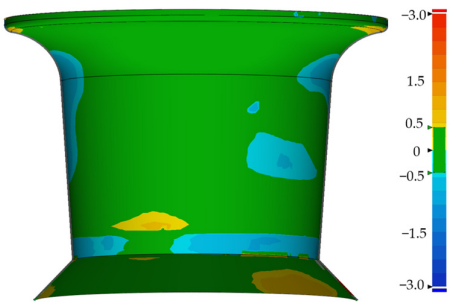	from −0.88 to 0.84

Table 5. *Cont.*

Name Details	Contours Deviations	Deviations from the Surface of the Polygonal Mesh, mm
Bottom	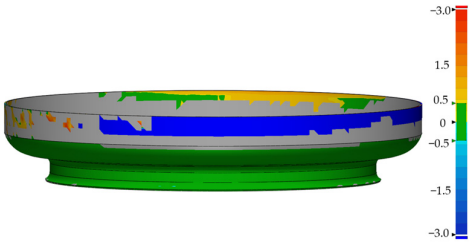	from −0.32 to 0.28
Pipe branch lower	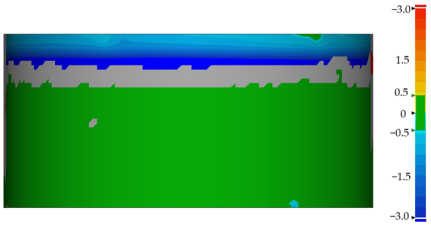	from −0.58 to 0.557
Funnel lower	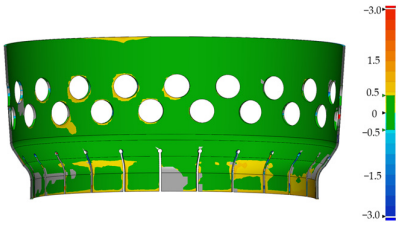	from 0.034 to 0.724
Shell (body)	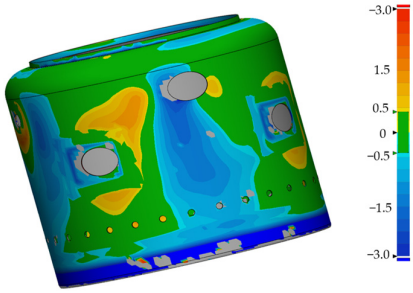	from −2.23 to 1.31

As a result of creating solid 3D models for the shell, funnel, bottom, lower branch pipe, and lower funnel parts, it was possible to achieve deviations from the grid surface not exceeding ±1 mm. These deviations are associated with the presence of various deformations that occurred during the operation of the combustion chamber, including thermal ones. The largest deviations from −2.23 to 1.31 mm occurred on the solid model of the outer shell of the combustion chamber. The lower part of the body (shell) was not completely scanned due to the bottom part, which partially covered it, as shown in Figure 15.

In this regard, when outputting the deviation diagram for a part of the body, its lower part is displayed in blue (has a deviation of less than 3 mm). By analogy, the parts of the lower and bottom pipes were also partially not scanned, since they were closed from the outside.

Due to a previously identified defect near the injector holes, deviations of the mesh from the solid geometry were analyzed, as shown in Figure 16.

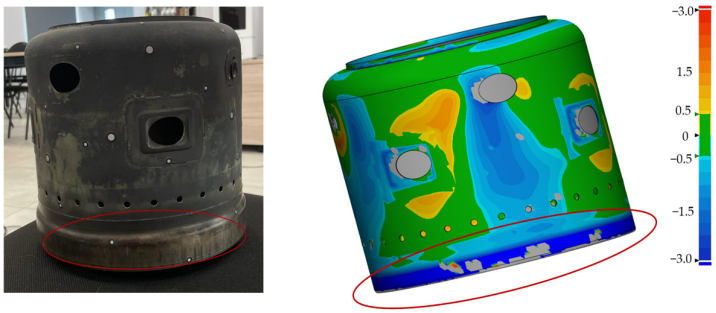

(**a**) (**b**)

Figure 15. Solid 3D model of the combustion chamber housing of the Capstone micro-GTU C 65 (Areas of greatest deviations highlighted in red): (**a**) shell (body) detail on the combustion chamber body; (**b**) the largest deviation of the shell (body) part from the polygonal model.

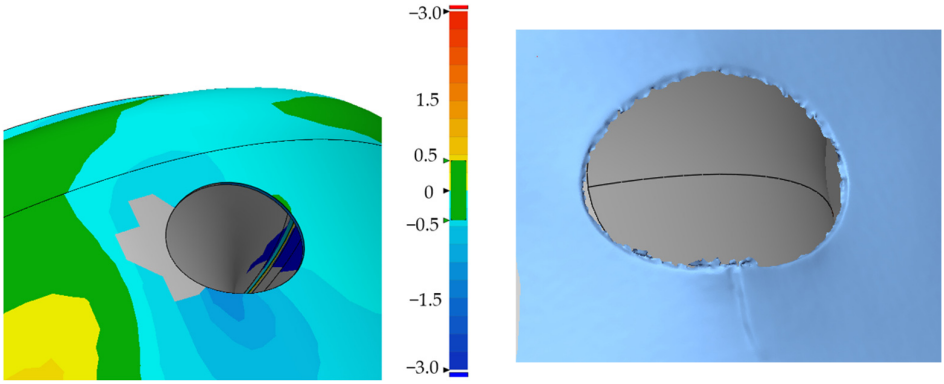

(**a**) (**b**)

Figure 16. Solid 3D model of the combustion chamber housing of the Capstone micro-GTU C 65: (**a**) dimensional deviation of the solid model shell (body) at the defect site; (**b**) the surface of the polygonal model at the site of the defect.

Since the sketches were made relative to the part of the lower shell, a deviation of solid-state geometry equal to −1.23 to −3.015 mm was observed at the site of the defect. Defects on the injector holes have also been replaced on the scanned surface of the polygonal grid.

After receiving all solid 3D models of the components of the combustion chamber housing of the Capstone C 65 micro-GTU, while maintaining the smallest deviation from the surface of the polygonal grid, the final appearance of the solid 3D model of the combustion chamber housing of the Capstone C 65 micro-GTU was obtained. Then, based on the obtained solid 3D model of the combustion chamber housing of the Capstone C 65 micro-GTU, the draft design documentation was developed.

Application of the described methodology to obtain solid-state 3D models and preliminary design documentation is possible for various units of the Capstone C 65 micro-GTU installation with a complex shape including a part of the gas turbine rotor, as shown in Figure 17.

Figure 17. Detail of the rotor of the gas turbine of the Capstone C 65 micro-GTU installation.

3.3. Comparison of the Obtained Dimensions of Solid-State Models with the Dimensions of the Prototype Combustion Chamber of the Capstone C 65 Micro-GTU

To validate the results obtained, it was necessary to compare the geometric characteristics of the developed solid-state model of the Capstone C 65 micro-GTU combustion chamber with the dimensions of the prototype. For this purpose, a measuring tool was used—a caliper with an error of 0.05 mm. With the help of the available caliper, it is possible to obtain the dimensions of the parts not exceeding 150 mm. Due to the described limitation, mixing and cooling holes were selected to determine the dimensional deviations, as well as details of the plates of the injector plates, the platinum of the spark plug, and the outer diameter of the pipe branch lower part.

Initially, measurements of the mixing and cooling holes were made. When measuring the prototype part, it was determined that the size for the mixing hole (D_{mix} = 5.65 mm) for the air-cooling holes was determined (D_c = 8.4 mm), as shown in Figure 18.

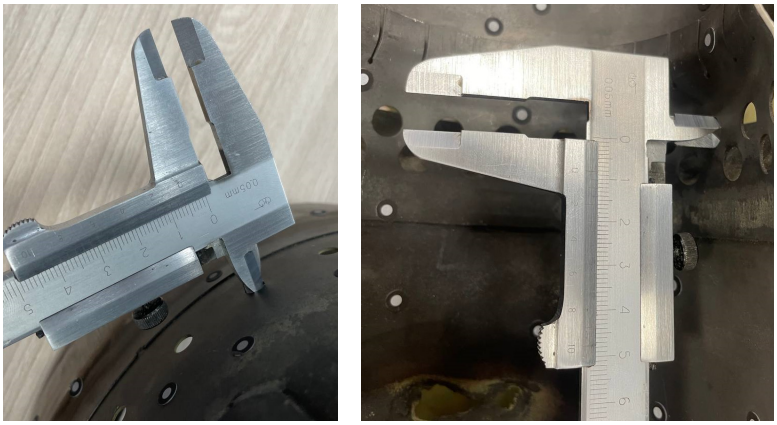

(**a**) (**b**)

Figure 18. Obtaining the geometric dimensions of the diameters of the cooling and mixing holes using a caliper: (**a**) measurement of mixing holes; (**b**) measuring the cooling holes.

Next, the size analysis was performed in the Geomagic Design X program due to the built-in software functions measure radius and measure distance. The sizes of the radius of the cooling holes (R_c = 2.855 mm) and mixing holes (R_{mix} = 4.318 mm) were obtained, as shown in Figure 19.

The dimensional deviations for the mixing and cooling holes were calculated using simple mathematical operations (1), (2):

$$|R_{mix} \times 2 - D_{mix}| = |2.855 \times 2 - 5.65| = 0.06 \text{ mm} \quad (1)$$

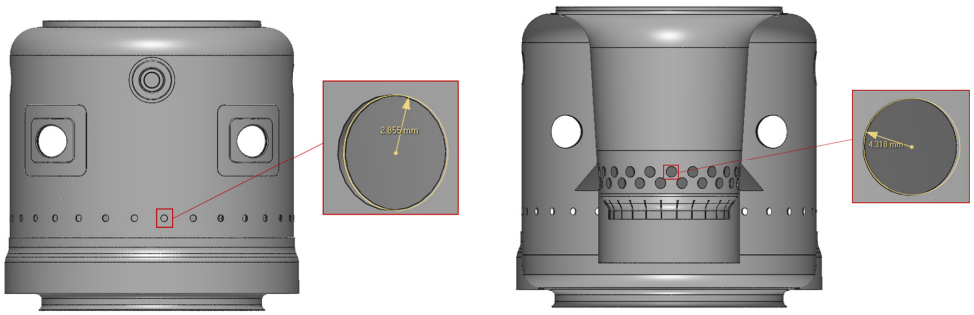

(**a**) (**b**)

Figure 19. The dimensions for the holes obtained as a result of the development of a solid-state model of the combustion chamber housing: (**a**) mixing hole size; (**b**) the size of the cooling hole.

R_{mix}—the radius of the mixing holes of the solid–state model; D_{mix}—the diameter of the mixing holes of the prototype combustion chamber housing.

$$|R_c \times 2 - D_c| = |4.318 \times 2 - 8.4| = 0.236 \text{ mm} \quad (2)$$

R_c—the radius of the cooling holes of the solid–state model; D_c—the diameter of the cooling holes of the prototype combustion chamber housing. Then, the dimensions of the plate with the injector hole, part of the spark plug, and the outer diameter of pipe branch lower were analyzed in a similar way. A comparison of the obtained dimensions and photos for each and the presented parts are presented in Table 6.

Table 6. Comparison of the dimensions of the parts of the Capstone C 65 micro-GTU combustion chamber prototype and the dimensions of the resulting 3D solid-state model.

Name Details	Dimensions Obtained Using a Caliper	Dimensions of the Developed Solid-State 3D Model	The Difference Between the Sizes, mm
Hole of the plate for the injector	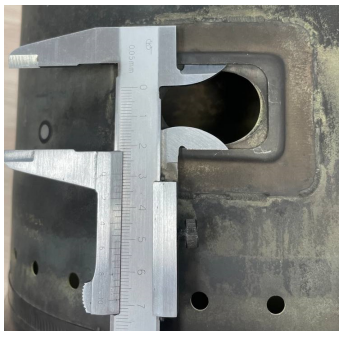 29.1 ± 0.05 mm	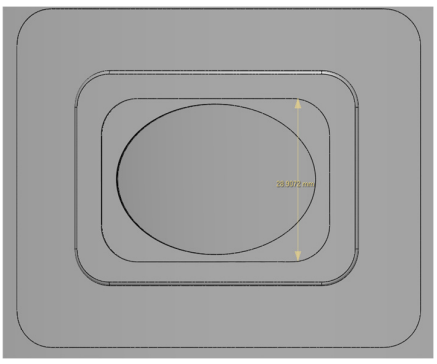 28.9072 mm	0.1928
	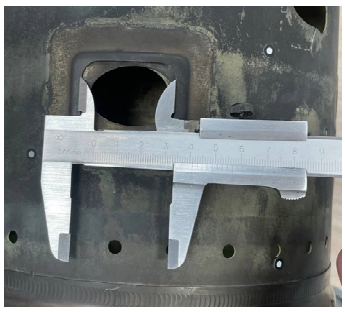 40.9 ± 0.05 mm	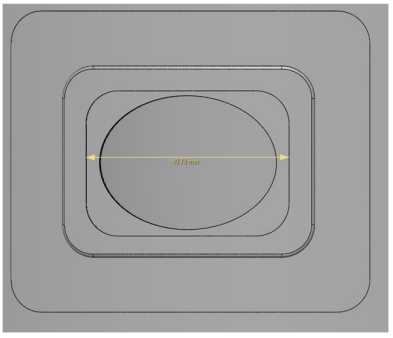 40.78 mm	0.12

Table 6. *Cont.*

Name Details	Dimensions Obtained Using a Caliper	Dimensions of the Developed Solid-State 3D Model	The Difference Between the Sizes, mm
Part of the locking spark plug	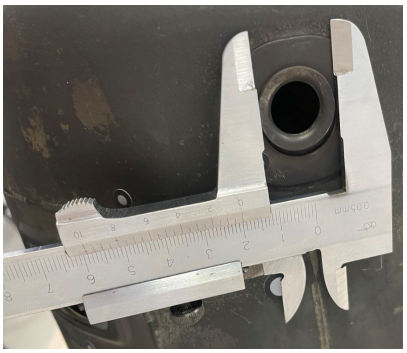 20 ± 0.05 mm	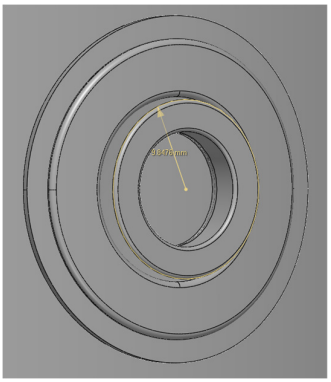 9.8476 × 2 = 19.6952 mm	0.3048
Pipe branch lower	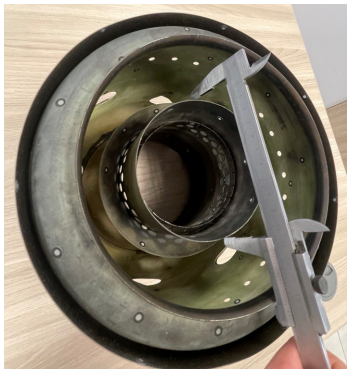 113.45 ± 0.05 mm	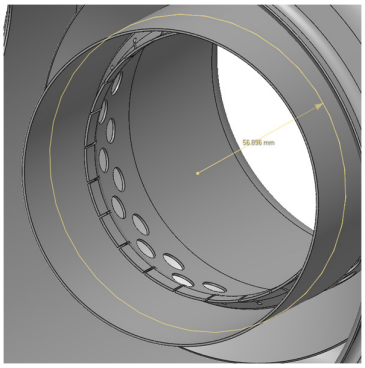 56.896 × 2 = 113.795 mm	0.345

Based on the comparison, dimensional deviations not exceeding 0.5 mm were obtained, which is sufficient for the parts of the combustion chamber housing components of the Capstone C 65 micro-GTU. To apply the methodology of developing a solid-state 3D model and preliminary design documentation to objects requiring greater dimensional accuracy, a smaller specified distance between points and more powerful PC equipment for data processing should be used.

4. Application of the Developed 3D Laser Scanning Methodology

To implement the developed methodology in the enterprise, it is necessary to perform several consecutive tasks. At the beginning, it is necessary to purchase equipment for the 3D scanning process, including a USD 33,000 FreeScan UE Pro 3D laser scanner, as well as equipment and software for processing and obtaining a cloud of scanned surface to obtain a polygonal model. Graviton D50A, worth USD 1750, was chosen as an example of PC hardware for data processing. As an example of a program for processing, the program Geomagic Design X license was selected, for which it costs more than USD 1900.

Next, it is necessary to train staff to complete the prototype preparation and 3D laser scanning process, which takes about 50 working hours on average.

After that, the staff must be trained to use the polygonal model processing program and develop the Geomagic Design X solid-state 3D model, which takes an average of 80 working hours. The time spent data were obtained as a result of training employees for the reverse engineering process using 3D scanning technology at the Department of Innovative Technologies of High-Tech Industries, National Research University "Moscow Power Engineering Institute". The time spent on training is presented in the form of a time cost diagram, shown in Figure 20.

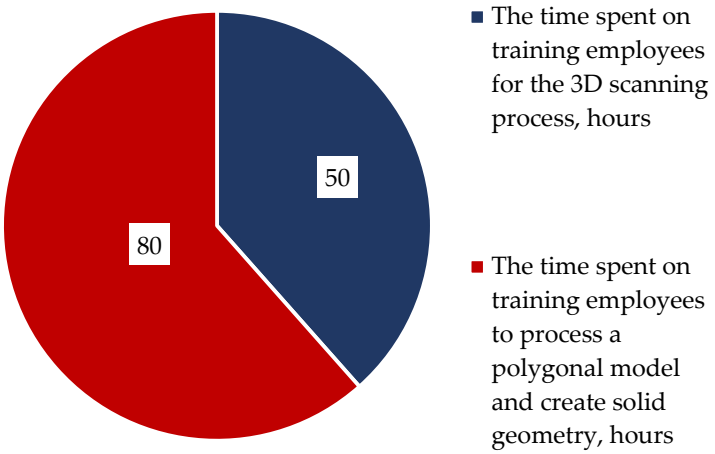

Figure 20. Diagram of the distribution of time spent on training employees in the reverse engineering process.

5. Conclusions

As a result of a comparative analysis of methods of contactless 3D scanning of parts, it was revealed that the most suitable method for obtaining a polygonal 3D model of the combustion chamber of the Capstone micro-GTU C 65 is a 3D laser scanning method due to its high precision characteristics.

The methodology for obtaining draft design documentation for the combustion chamber housing of the Capstone micro-GTU C 65 has been improved, based on obtaining its polygonal model using laser 3D scanning and its further processing in the Geomagic program Design X in order to obtain a solid 3D model.

Based on the conducted research, recommendations were developed for selecting 3D scanning settings in order to obtain highly detailed three-dimensional models of equipment parts that are objects of reverse engineering. The influence of 3D scanning settings on the geometric parameters of the solid 3D model was also estimated. It was determined that in order to reduce the time spent on scanning and processing by 1.5 times, the distance between the points of the polygonal grid should be selected from 0.35 to 0.2 mm. With limited computing power, for a smaller file size of the polygonal model, it is necessary to select in the range from 1 to 0.3 mm, since when the distance between the points is reduced by less than 0.3 mm, the file size increases more than 2 times.

The resulting methodology can be applied to other parts of micro-GTU assemblies, including parts of the rotor of a gas turbine. In the process of performing 3D scanning, the capacity limit of the PC equipment used for processing was determined, which amounted to 10,800.000 points. This limit should be taken into account when 3D scanning volumetric parts with dimensions greater than 250 × 250 × 250 mm.

For the implementation and use of the obtained methodology, the estimated material costs for the purchase of equipment and the total time for staff training were calculated. The total cost of 3D scanning equipment and PC processing equipment, including the license for the program, amounted to USD 36,650. Also, the cost of working time for staff training totaled 130 working hours. With limited computing power, for a smaller file size of the polygonal model, it is necessary to select in the range from 1 to 0.3 mm, since when the distance between the points is reduced by less than 0.3 mm, the file size increases more than two times.

Author Contributions: Conceptualization, S.O. and I.K.; methodology, O.Z.; software, G.G.; validation, O.Z.; formal analysis, S.O.; investigation, S.O. and I.K.; resources, O.Z.; data curation, A.V.; writing—original draft preparation, G.G.; writing—review and editing, S.O. and I.K.; visualization, A.V.; supervision, S.O.; project administration, O.Z.; funding acquisition, G.G. All authors have read and agreed to the published version of the manuscript.

Funding: This study conducted by Moscow Power Engineering Institute was financially supported by the Ministry of Science and Higher Education of the Russian Federation (project no. FSWF-2023-0014, contract no. 075-03-2023-383, 2023/18/01).

Data Availability Statement: Data are contained within the article.

Conflicts of Interest: The authors declare no conflicts of interest in terms of the collection, analyses, or interpretation of data; in the writing of the manuscript; or in the decision to publish the results.

References

1. Chichirova, N.D.; Filimonova, A.A.; Cherkasov, A.S.; Lyapin, A.I. Overview of the Possibility of Using Low-Power Gas Turbines. *J. Sib. Fed. Univ. Eng. Technol.* **2023**, *16*, 584–600.
2. Vikulov, O.V.; Rybakov, Y.L. Gas Microturbines as a Promising Product of Conversion of Military Engine Building. *Innov. Expert. Sci. Pap.* **2021**, 160–167. [CrossRef]
3. GOST R 57558-2017 | NATIONAL STANDARDS. Available online: https://protect.gost.ru/document.aspx?control=7&id=218140 (accessed on 13 September 2024).
4. Haleem, A.; Javaid, M. Additive manufacturing applications in industry 4.0: A review. *J. Ind. Integr. Manag.* **2019**, *4*, 1930001. [CrossRef]
5. Ali, A.; Soni, M.; Javaid, M.; Haleem, A. A Comparative Analysis of Different Rapid Prototyping Techniques for Making Intricately Shaped Structure. *J. Ind. Integr. Manag.* **2020**, *05*, 393–407. [CrossRef]
6. Javaid, M.; Haleem, A. 3D Printed Tissue and Organ Using Additive Manufacturing: An Overview. *Clin. Epidemiol. Glob. Health* **2020**, *8*, 586–594. [CrossRef]
7. Haleem, A.; Gupta, P.; Bahl, S.; Javaid, M.; Kumar, L. 3D Scanning of a Carburetor Body Using COMET 3D Scanner Supported by COLIN 3D Software: Issues and Solutions. *Mater. Today Proc.* **2021**, *39*, 331–337. [CrossRef] [PubMed]
8. Li, T.; Polette, A.; Lou, R.; Jubert, M.; Nozais, D.; Pernot, J.-P. Machine learning-based 3D scan coverage prediction for smart-control applications. *Comput.-Aided Des.* **2024**, *176*, 103775. [CrossRef]
9. Tootooni, M.S.; Dsouza, A.; Donovan, R.; Rao, P.K.; Kong, Z.; Borgesen, P. Classifying the dimensional variation in additive manufactured parts from laser-scanned three-dimensional point cloud data using machine learning approaches. *J. Manuf. Sci. Eng.* **2017**, *139*, 091005. [CrossRef]
10. Peng, Y.; Wang, Y.; Hu, F.; He, M.; Mao, Z.; Huang, X.; Ding, J. Predictive modeling of flexible EHD pumps using kolmogorov-arnold networks. *arXiv* **2024**, arXiv:2405.07488. [CrossRef]
11. Šagi, G.; Lulić, Z.; Mahalec, I. Reverse Engineering. Concurrent Engineering in the 21st Century. In *Foundations, Developments and Challenges*; Springer: Berlin/Heidelberg, Germany, 2015; pp. 319–353.
12. Gerbino, S.; Martorelli, M. Reverse Engineering. In *Springer Handbook of Additive Manufacturing*; Springer: Berlin/Heidelberg, Germany, 2023; pp. 253–268.
13. Sierra, J.; Correa, E. Obtaining the CAD Flow Models in the Francis Turbine of the Sancancio Hydroelectric Power Plant by Means of Reverse Engineering. *Int. J. Integr. Eng.* **2020**, *12*, 172–187.
14. Ulucak, O. Rehabilitation of Old Francis Turbines Using Reverse Engineering and Computational Fluid Dynamics Simulations. Master's Thesis, Çankaya Üniversitesi, Ankara, Turkey, 2020.
15. Bondyra, R.; Dominiczak, K.; Matuszak, J. Reverse Engineering Methodology as a Way of Steam Turbine Blades Designing for Loviisa Nuclear Power. *E3S Web Conf.* **2019**, *137*, 01002. [CrossRef]
16. Arailopoulos, A.; Giagopoulos, D.; Zacharakis, I.; Pipili, E. Integrated Reverse Engineering Strategy for Large-Scale Mechanical Systems: Application to a Steam Turbine Rotor. *Front. Built Environ.* **2018**, *4*, 55. [CrossRef]
17. Fivaz, M.; Van der Spuy, J.; Van Eck, H. The Effect of Compressor Stage Impeller Gap Tolerances on the Performance of a Solarised Micro Gas Turbine. 2024. Available online: https://assets-eu.researchsquare.com/files/rs-3833813/v1_covered_7119c3e6-5229-4b12-ac7b-0a2b11f03a40.pdf (accessed on 23 September 2024).
18. Capstone Green Energy Corporation (CGRNQ). Available online: https://www.capstonegreenenergy.com/products/capstone-microturbines/c65 (accessed on 13 September 2024).
19. Osipov, S.K.; Gertsovsky, G.A.; Mechnik, D.A.; Chechetkin, D.A.; Pukhov, A.V. Reverse Engineering of the Combustion Chamber of a Capstone C60 Micro-GTU. *New Russ. Electr. Power Ind.* **2024**, 6–13. Available online: https://elibrary.ru/dervgt (accessed on 10 September 2024).
20. FreeScan UE Pro: Laser Handheld 3D Scanner SHINING 3D. Available online: https://www.shining3d.ru/solutions/freescan-ue-pro/ (accessed on 3 April 2024).

21. Kaiser, J.; Dědič, M. Influence of Material on the Density of a Point Cloud Created Using a Structured-Light 3D Scanner. *Appl. Sci.* **2024**, *14*, 1476. [CrossRef]
22. Legal Information Institute U.S. Code § 206—Standard Gauge for Sheet and Plate Iron and Steel. Available online: https://www.law.cornell.edu/uscode/text/15/206 (accessed on 10 September 2024).